Analytical model of resonant electromagnetic dipole-quadrupole coupling in nanoparticle arrays

Viktoriia E. Babicheva[1,*] and Andrey B. Evlyukhin[2,†]

[1]*University of Arizona, College of Optical Sciences, Tucson, Arizona 85721, USA*
[2]*Institute of Quantum Optics, Leibniz Universität Hannover, 30167 Hannover, Germany*

An analytical model for investigations of multipole coupling effects in the finite and infinite nanoparticle arrays supporting electromagnetic resonances is presented and discussed. This model considers the contributions of both electric and magnetic modes excited in the nanoparticles, including electric and magnetic dipoles and electric and magnetic quadrupoles. The magnetic quadrupole propagator (Green's tensor) that describes the electromagnetic field generated by a point magnetic quadrupole source in all wave zones is derived. As an example, we apply the developed model to study infinite two-dimensional rectangular periodic arrays of spherical silicon nanoparticles supporting the dipole and quadrupole resonant responses. The correctness and accuracy of the analytical model are confirmed by the agreement of its results with the results of full-wave numerical simulations. Using the developed model, we show the electromagnetic coupling between electric dipole and magnetic quadrupole moments as well as between magnetic dipole and electric quadrupole moments even for the case of an infinite rectangular periodic array of spherical nanoparticles. The strong suppression of the dipole or quadrupole moment due to the coupling effects is demonstrated and discussed for spherical nanoparticle arrays. The analytical expressions for the reflection and transmission coefficients written with the effective dipole and quadrupole polarizabilities are derived for normal light incidences and zero-order diffraction. The derived expressions are applied to explain the lattice anapole (invisibility) states when the incident light is transmitted unperturbed through the silicon nanoparticle array. The important role of dipole and quadrupole excitations in scattering compensation resulting in the lattice anapole effect is explicitly demonstrated. The presented approach can be used for designing metasurfaces and further utilizing them in developing ultrathin functional optical elements.

I. INTRODUCTION

Nanostructures have demonstrated a great potential to be utilized in optical applications and photonic devices, with particular interest in photovoltaics [1], sensing [2], flat functional elements (e.g., based on metasurfaces) [3–5], enhanced photoemission [6], near-field microscopy [7], and others. Different materials with negative [8,9], positive [10,11], and undefined [12] permittivity and nanoparticle shapes have been explored with the aim to enhance light-matter interaction in the nanostructure [8–12]. Nanocomposites, including core-shell nanoparticles, allow for excitation of various multipole resonances and precise control of nanostructures' scattering and absorption properties [13–16].

The strong magnetic response of the nanostructures is crucial for efficient control of light at the nanoscale. In the visible and infrared spectral ranges, materials have a very weak magnetic response, and nanostructures need to be designed to possess not only electric resonances but also artificial magnetic ones. To induce the artificial magnetic response in metallic (plasmonic) particles, one has to use U-shaped particles, split-ring resonators, or a similar shape, and fabrication of such metallic particles imposes severe limitations on their practical implementations. Recently, dielectrics with a high refractive index (e.g., semiconductors such as silicon, germanium, and III-V compounds) have attracted a lot of attention because particles with the relatively simple shape, such as a sphere or a disk, have shown that they can support both electric and magnetic resonances [10,17]. Interplay and overlap of resonances in such high-index particles offer the possibility to effectively control light at subwavelength dimensions and design ultrathin photonic elements based on such antennas and their arrays [18–24].

Being arranged in the lattice, particles interact with each other, and their effective polarizabilities are defined not only by the properties of the individual particle but all particles in the array as well as the distance between them [25–28]. Periodic arrays of nanoparticles enable excitation of additional resonance, so-called lattice resonance, that appears in proximity to the Rayleigh anomaly (wavelength of diffraction) [29–36]. Different particle multipoles respond differently to the change in the lattice period in a particular direction and incident light polarization [10,37]. It has been shown that one can independently control electric and magnetic dipole resonances in the rectangular periodic lattice and achieve resonance overlap [38,39]. Analytical models for the infinite rectangular periodic array based on coupled dipole equations show that electric and magnetic dipoles do not couple [10], which is similar to the case of a single particle without an array. Likewise, an electric dipole does not couple to an

*vbb@unm.edu
†a.b.evlyukhin@daad-alumni.de

electric quadrupole [37]. However, a magnetic dipole couples to an electric quadrupole [40,41], and this coupling brings about interesting effects that are enabled by the lattice (see, e.g., the demonstration of the generalized Kerker effect in Ref. [40]).

Here we take the next step in the analysis of nanostructure properties with electric and magnetic multipole resonances. We take into consideration both electric and magnetic responses of the particle for dipole and quadrupole moments, and we focus mainly on the magnetic quadrupole response of the nanoparticles. We study the effects stemming from including the magnetic quadrupole moment in both cases of single-particle and rectangular periodic array arrangement. First, we derive the magnetic quadrupole propagator (Green's tensor) and show how electromagnetic fields are defined through this tensor. Second, we derive the equations for an array of nanoparticles with the electric and magnetic dipole and quadrupole responses in a general case of arbitrary nanoparticles (different from each other in terms of size, shape, material, position in the array, etc.).

Consideration of a general case of arbitrary nanoparticle arrangement is followed by a study of a particular case of an infinite rectangular periodic array of identical spheres. We introduce effective polarizabilities of each multipole of the identical nanoparticles in the rectangular periodic array, and we derive their expressions, which include terms responsible for coupling between the electric dipole and the magnetic quadrupole as well as reflection and transmission coefficients of the array. Our results show that it is important to take into account excitation of the magnetic quadrupole moment in the nanoparticle lattice: (i) if magnetic quadrupole polarizability is negligible for a single particle, it can be significant in the lattice because of its coupling to the electric dipole; and (ii) non-negligible magnetic quadrupole polarizability changes an electric dipole. Finally, we show that it is possible to achieve a condition when particle multipoles are excited, but the transmitted wave changes neither the amplitude nor the phase. Thus, we show the origin of the lattice anapole effect. We would like to emphasize that this effect is different from the perfect transmission in metalattices and metasurfaces occurring when electric and magnetic dipoles compensate for each other's scattering and the first Kerker condition is satisfied [18]. It is often referred to as the Kerker effect, it manifests only as a suppression of backward scattering, and the phase difference for the incident and transmitted waves can be arbitrary [42].

One of the main results of our work is the explicit demonstration of the coupling effects between the electric dipole and magnetic quadrupole moments of the identical nanoparticles arranged in the infinite rectangular array. In contrast to our previous work [40], which was devoted to the coupling between electric and magnetic multipoles of the same order (magnetic dipole to electric quadrupole coupling), here we demonstrate the electromagnetic coupling between multipoles of different orders. In our work, we show that under the condition of the resonant dipole and quadrupole nanoparticle responses, their coupling can play a crucial role, strongly affect effective polarizability of both multipoles, and define spectral features in transmission, reflection, and absorption in the array.

II. ELECTRIC AND MAGNETIC FIELDS OF MULTIPOLES

In the multipole approximation, including the dipole and quadrupole moments, nanoparticles are considered as point electric and magnetic dipoles (ED and MD) and point electric and magnetic quadrupoles (EQ and MQ). The analytical expressions for the electric and magnetic fields generated by point electric and magnetic dipoles and electric quadrupoles are considered elsewhere [10,17]. Here we obtain the expressions for the electric and magnetic fields generated by the point magnetic quadrupole source. In general, the presented procedure can be applied to calculate field propagators of any multipole moments. For example, using this approach the field propagator for an electric toroidal dipole has been calculated in Ref. [43].

A. Magnetic quadrupole propagator

The electric field propagator of multipole sources can be obtained from the general expression for the electric field **E** generated at a space point **r** by polarization **P** excited in a local region with volume V_s [44]:

$$\mathbf{E}(\mathbf{r}) = \frac{k_0^2}{\varepsilon_0} \int_{V_s} \hat{G}(\mathbf{r}, \mathbf{r}')\mathbf{P}(\mathbf{r}')d\mathbf{r}', \tag{1}$$

where k_0 is the wave number in vacuum, ε_0 is the vacuum dielectric constant, and $\hat{G}(\mathbf{r}, \mathbf{r}')$ is the Green's tensor of the system without the polarization **P** (see Refs. [10,45]). The multipole decomposition of the induced polarization **P** up to the magnetic quadrupole term can be written as [43]

$$\mathbf{P}(\mathbf{r}') \simeq \mathbf{p}\delta(\mathbf{r}'') - \frac{1}{6}\hat{Q}\nabla\delta(\mathbf{r}'') + \frac{i}{\omega}[\nabla \times \mathbf{m}\delta(\mathbf{r}'')]$$
$$- \frac{i}{2\omega}[\nabla \times \hat{M}\nabla\delta(\mathbf{r}'')] + \cdots, \tag{2}$$

where $\delta(\mathbf{r}'')$ is the Dirac delta function, $\mathbf{r}'' = \mathbf{r}' - \mathbf{r}_0$ ($\mathbf{r}_0$ is the radius-vector of the multipoles' location), ∇ is the gradient operator with respect to the radius-vector $\mathbf{r}'$, ω is the angular frequency [here we consider monochromatic time dependence $\exp(-i\omega t)$], and the values **p**, **m**, $\hat{Q}$, and $\hat{M}$ are the electric dipole vector, magnetic dipole vector, electric quadrupole tensor, and magnetic quadrupole tensor, respectively. Inserting Eq. (2) into (1) and considering every term separately, one can obtain the electric field generated by every multipole in all wave zones. The fields generated by the dipoles and the electric quadrupole are considered elsewhere [10,17,37], and the results will be used in the following sections. The field generated by the magnetic quadrupole tensor $\hat{M}$ is calculated from the following equation:

$$\mathbf{E}^M(\mathbf{r}) = -\frac{ik_0^2}{2\varepsilon_0\omega} \int_{V_s} \hat{G}(\mathbf{r}, \mathbf{r}')[\nabla \times \hat{M}\nabla\delta(\mathbf{r}' - \mathbf{r}_0)]d\mathbf{r}'. \tag{3}$$

After integration of (3), taking into account that the tensor $\hat{M}$ is traceless ($M_{xx} + M_{yy} + M_{zz} = 0$) and symmetric ($M_{xy} = M_{yx}$, $M_{xz} = M_{zx}$, $M_{yz} = M_{zy}$), and the Green's tensor $\hat{G}(\mathbf{r}, \mathbf{r}')$ corresponds to a homogeneous medium with ε_S [43,45], one obtains, for the local electric field at a point $\mathbf{r}_l$ generated by

the $\hat{M}$ source located at a point $\mathbf{r}_j$, the following expression:

$$\mathbf{E}^M(\mathbf{r}_l) = \frac{ik_0 k_S^2}{2}\sqrt{\frac{\mu_0}{\varepsilon_0}}\frac{e^{ik_S R_{lj}}}{4\pi R_{lj}}\left(1 + \frac{3i}{k_S R_{lj}} - \frac{3}{k_S^2 R_{lj}^2}\right)$$

$$[\mathbf{n}_{jl} \times (\hat{M}\mathbf{n}_{jl})], \qquad (4)$$

where $\mathbf{n}_{jl} = (\mathbf{r}_l - \mathbf{r}_j)/|\mathbf{r}_l - \mathbf{r}_j|$ is the unit vector directed from $\mathbf{r}_j$ to $\mathbf{r}_l$, i is the imaginary unit, $\mathbf{R}_{lj} = \mathbf{r}_l - \mathbf{r}_j$, $R_{lj} = |\mathbf{R}_{lj}|$, μ_0 is the vacuum permeability, $k_S = k_0\sqrt{\varepsilon_S}$, and the sign $\times$ denotes the vector product between corresponding vectors.

The expression (4) can be presented as

$$\mathbf{E}^M(\mathbf{r}_l) = \left[\mathbf{G}_{lj}^M \times (\hat{M}\mathbf{n}_{jl})\right], \qquad (5)$$

where the vector

$$\mathbf{G}_{lj}^M = \frac{ik_0 k_S^2}{2}\sqrt{\frac{\mu_0}{\varepsilon_0}}\frac{e^{ik_S R_{lj}}}{4\pi R_{lj}^2}\left(1 + \frac{3i}{k_S R_{lj}} - \frac{3}{k_S^2 R_{lj}^2}\right)\mathbf{R}_{lj} \quad (6)$$

is the magnetic quadrupole propagator. From Maxwell equations, the magnetic field can be found as

$$\mathbf{H}^M(\mathbf{r}_l) = \frac{c\varepsilon_0}{ik_0}\nabla \times \mathbf{E}^M(\mathbf{r}_l) \qquad (7)$$

and correspondingly defined through the propagator $\hat{G}_{lj}^M$ as

$$\mathbf{H}^M(\mathbf{r}_l) = k_S^2 \hat{G}_{lj}^M(\hat{M}\mathbf{n}_{jl}), \qquad (8)$$

where, after derivations, the magnetic quadrupole Green's tensor of the medium without particles is

$$\hat{G}_{lj}^M \equiv \frac{i3k_S e^{ik_S R_{lj}}}{24\pi R_{lj}}\left[\left(-1 - \frac{i3}{k_S R_{lj}} + \frac{6}{k_S^2 R_{lj}^2} + \frac{i6}{k_S^3 R_{lj}^3}\right)\hat{U} \right.$$

$$\left. + \left(1 + \frac{i6}{k_S R_{lj}} - \frac{15}{k_S^2 R_{lj}^2} - \frac{i15}{k_S^3 R_{lj}^3}\right)\mathbf{n}_{jl}\mathbf{n}_{jl}\right], \qquad (9)$$

where $\hat{U}$ is the 3×3 unit tensor, and $\mathbf{n}_{jl}\mathbf{n}_{jl}$ is the dyadic product.

B. Electric and magnetic fields of dipole and quadrupole sources

Here we present general expressions for electric and magnetic fields generated by dipole and quadrupole point sources. The electric dipole and electric quadrupole Green's tensors of the medium without particles are defined as (see the previous works [10,37])

$$\hat{G}_{lj}^p \equiv \left\{\left(1 + \frac{i}{k_S R_{lj}} - \frac{1}{k_S^2 R_{lj}^2}\right)\hat{U} + \left(-1 - \frac{i3}{k_S R_{lj}} + \frac{3}{k_S^2 R_{lj}^2}\right)\mathbf{n}_{jl}\mathbf{n}_{jl}\right\}\frac{e^{ik_S R_{lj}}}{4\pi R_{lj}} \qquad (10)$$

and

$$\hat{G}_{lj}^Q \equiv \frac{ik_S e^{ik_S R_{lj}}}{24\pi R_{lj}}\left\{\left(-1 - \frac{i3}{k_S R_{lj}} + \frac{6}{k_S^2 R_{lj}^2} + \frac{i6}{k_S^3 R_{lj}^3}\right)\hat{U} + \left(1 + \frac{i6}{k_S R_{lj}} - \frac{15}{k_S^2 R_{lj}^2} - \frac{i15}{k_S^3 R_{lj}^3}\right)\mathbf{n}_{jl}\mathbf{n}_{jl}\right\}, \qquad (11)$$

respectively. We take into account that tensors $\hat{Q}$ and $\hat{M}$ are traceless and symmetric and that

$$\hat{G}_{lj}^m = \hat{G}_{lj}^p, \qquad \hat{G}_{lj}^M = 3\hat{G}_{lj}^Q, \qquad (12)$$

where $\hat{G}_{lj}^m$ is the tensor determining the magnetic field at the point $\mathbf{r}_l$ generated by a magnetic dipole located at the point $\mathbf{r}_j$. In this case, one can express electric and magnetic fields of multipoles as the following:

$$\mathbf{E}^p(\mathbf{r}_l) = \frac{k_0^2}{\varepsilon_0}\hat{G}_{lj}^p \mathbf{p}^j,$$

$$\mathbf{H}^p(\mathbf{r}_l) = \frac{ck_0}{i}\nabla \times \hat{G}_{lj}^p \mathbf{p}^j = \frac{ck_0}{i}[\mathbf{g}_{lj} \times \mathbf{p}^j], \qquad (13)$$

$$\mathbf{H}^m(\mathbf{r}_l) = k_S^2 \hat{G}_{lj}^p \mathbf{m}^j,$$

$$\mathbf{E}^m(\mathbf{r}_l) = \frac{ik_0}{c\varepsilon_0}\nabla \times \hat{G}_{lj}^p \mathbf{m}^j = \frac{ik_0}{c\varepsilon_0}[\mathbf{g}_{lj} \times \mathbf{m}^j], \qquad (14)$$

$$\mathbf{E}^Q(\mathbf{r}_l) = \frac{k_0^2}{\varepsilon_0}\hat{G}_{lj}^Q(\hat{Q}^j\mathbf{n}_{jl}),$$

$$\mathbf{H}^Q(\mathbf{r}_l) = \frac{ck_0}{i}\nabla \times \hat{G}_{lj}^Q(\hat{Q}^j\mathbf{n}_{jl}) = \frac{ck_0}{i}[\mathbf{q}_{lj} \times (\hat{Q}^j\mathbf{n}_{jl})], \qquad (15)$$

$$\mathbf{H}^M(\mathbf{r}_l) = k_S^2 \hat{G}_{lj}^M(\hat{M}^j\mathbf{n}_{jl}) = 3k_S^2 \hat{G}_{lj}^Q(\hat{M}^j\mathbf{n}_{jl}), \qquad (16)$$

$$\mathbf{E}^M(\mathbf{r}_l) = \frac{ik_0}{c\varepsilon_0}\nabla \times \hat{G}_{lj}^M(\hat{M}^j\mathbf{n}_{jl}) = 3\frac{ik_0}{c\varepsilon_0}\nabla \times \hat{G}_{lj}^Q(\hat{M}^j\mathbf{n}_{jl})$$

$$= 3\frac{ik_0}{c\varepsilon_0}[\mathbf{q}_{lj} \times (\hat{M}^j\mathbf{n}_{jl})],$$

where $c = 1/\sqrt{\varepsilon_0\mu_0}$ is the speed of light in vacuum; the introduced (for convenience) vectors $\mathbf{g}_{lj}$ and $\mathbf{q}_{lj}$ are

$$\mathbf{g}_{lj} = \frac{e^{ik_S R_{lj}}}{4\pi R_{lj}}\left(\frac{ik_S}{R_{lj}} - \frac{1}{R_{lj}^2}\right)\mathbf{R}_{lj} \qquad (17)$$

and

$$\mathbf{q}_{lj} = \frac{c\varepsilon_0}{3ik_0}\mathbf{G}_{lj}^M = \frac{k_S^2 e^{ik_S R_{lj}}}{24\pi R_{lj}^2}\left(1 + \frac{3i}{k_S R_{lj}} - \frac{3}{k_S^2 R_{lj}^2}\right)\mathbf{R}_{lj}. \qquad (18)$$

The connection between $\mathbf{q}_{lj}$ and $\mathbf{G}_{lj}^M$ follows from Eqs. (5), (6), and (16).

III. MULTIPOLAR NANOPARTICLE STRUCTURES

A. General system of equations

Let us consider an arbitrarily shaped particle with number j in the structure of N identical particles with ED, MD, EQ, and MQ polarizability tensors $\hat{\alpha}_p$, $\hat{\alpha}_m$, $\hat{\alpha}_Q$, and $\hat{\alpha}_M$, respectively. The vectors of the electric $\mathbf{p}^j$ and magnetic $\mathbf{m}^j$ dipole moments and the tensors of the electric $\hat{Q}^j$ and

magnetic $\hat{M}^j$ quadrupole moments at the particle location $\mathbf{r}_j$ are proportional to the local electric $\mathbf{E}^{\text{loc}}(\mathbf{r}_j)$ and magnetic $\mathbf{H}^{\text{loc}}(\mathbf{r}_j)$ fields and symmetrical parts of the gradients of the local electric or magnetic field, respectively:

$$\mathbf{p}^j = \hat{\alpha}_p \mathbf{E}^{\text{loc}}(\mathbf{r}_j), \tag{19}$$

$$\mathbf{m}^j = \hat{\alpha}_m \mathbf{H}^{\text{loc}}(\mathbf{r}_j), \tag{20}$$

$$\hat{Q}^j = \frac{\hat{\alpha}_Q}{2}[\nabla \mathbf{E}^{\text{loc}}(\mathbf{r}_j) + \mathbf{E}^{\text{loc}}(\mathbf{r}_j)\nabla], \tag{21}$$

$$\hat{M}^j = \frac{\hat{\alpha}_M}{2}[\nabla \mathbf{H}^{\text{loc}}(\mathbf{r}_j) + \mathbf{H}^{\text{loc}}(\mathbf{r}_j)\nabla], \tag{22}$$

where ∇ is the nabla operator. For tensorial terms, we use the convention [46] to define tensor elements $\nabla\mathbf{F} + \mathbf{F}\nabla$ in a Cartesian coordinate system as

$$(\nabla\mathbf{F} + \mathbf{F}\nabla)_{\beta\gamma} = \frac{\partial F_\gamma}{\partial \beta} + \frac{\partial F_\beta}{\partial \gamma},$$

where $\mathbf{F}$ is a vector of the electric or magnetic field, $\beta = x, y, z$, and $\gamma = x, y, z$.

For the particle located at the position $\mathbf{r}_j$, the local electric field is a superposition of the external electric $\mathbf{E}_0(\mathbf{r}_j)$, the field $\tilde{\mathbf{E}}^p(\mathbf{r}_j)$ produced by all EDs of the system except $\mathbf{p}^j$, the field $\tilde{\mathbf{E}}^m(\mathbf{r}_j)$ of all MDs except $\mathbf{m}^j$, the field $\tilde{\mathbf{E}}^Q(\mathbf{r}_j)$ of all EQs except $\hat{Q}^j$, and the field $\tilde{\mathbf{E}}^M(\mathbf{r}_j)$ of all MQs except $\hat{M}^j$; the same considerations are applied to the magnetic field:

$$\mathbf{E}^{\text{loc}}(\mathbf{r}_j) = \mathbf{E}_0(\mathbf{r}_j) + \tilde{\mathbf{E}}^p(\mathbf{r}_j) + \tilde{\mathbf{E}}^m(\mathbf{r}_j)$$
$$+ \tilde{\mathbf{E}}^Q(\mathbf{r}_j) + \tilde{\mathbf{E}}^M(\mathbf{r}_j), \tag{23}$$

$$\mathbf{H}^{\text{loc}}(\mathbf{r}_j) = \mathbf{H}_0(\mathbf{r}_j) + \tilde{\mathbf{H}}^p(\mathbf{r}_j) + \tilde{\mathbf{H}}^m(\mathbf{r}_j)$$
$$+ \tilde{\mathbf{H}}^Q(\mathbf{r}_j) + \tilde{\mathbf{H}}^M(\mathbf{r}_j). \tag{24}$$

Using the exact expressions (13)–(16) for electromagnetic fields generated by dipole and quadrupole sources, the equation system (19)–(22) for calculation of the dipole and quadrupole moments of all particles can be written in a more explicit form:

$$\mathbf{p}^j = \hat{\alpha}_p \mathbf{E}_0(\mathbf{r}_j) + \hat{\alpha}_p \frac{k_0^2}{\varepsilon_0} \sum_{l \neq j}^N \left\{ \hat{G}_{jl}^p \mathbf{p}^l + \frac{i}{ck_0}[\mathbf{g}_{jl} \times \mathbf{m}^l] \right.$$
$$\left. + \hat{G}_{jl}^Q(\hat{Q}^l \mathbf{n}_{lj}) + \frac{3i}{ck_0}[\mathbf{q}_{jl} \times (\hat{M}^l \mathbf{n}_{lj})] \right\},$$

$$\mathbf{m}^j = \hat{\alpha}_m \mathbf{H}_0(\mathbf{r}_j) + \hat{\alpha}_m k_0^2 \sum_{l \neq j}^N \left\{ \frac{c}{ik_0}[\mathbf{g}_{jl} \times \mathbf{p}^l] + \varepsilon_S \hat{G}_{jl}^p \mathbf{m}^l \right.$$
$$\left. + \frac{c}{ik_0}[\mathbf{q}_{jl} \times (\hat{Q}^l \mathbf{n}_{lj})] + 3\varepsilon_S \hat{G}_{jl}^Q(\hat{M}^l \mathbf{n}_{lj}) \right\},$$

$$\hat{Q}^j = \frac{\hat{\alpha}_Q}{2}[\nabla \mathbf{E}_0(\mathbf{r}_j) + \mathbf{E}_0(\mathbf{r}_j)\nabla]$$
$$+ \frac{\hat{\alpha}_Q k_0^2}{2\varepsilon_0} \sum_{l \neq j}^N \left\{ [\nabla_j(\hat{G}_{jl}^p \mathbf{p}^l) + (\hat{G}_{jl}^p \mathbf{p}^l)\nabla_j] \right.$$

$$+ \frac{i}{ck_0}(\nabla_j[\mathbf{g}_{jl} \times \mathbf{m}^l] + [\mathbf{g}_{jl} \times \mathbf{m}^l]\nabla_j)$$
$$+ \{\nabla_j[\hat{G}_{jl}^Q(\hat{Q}^l \mathbf{n}_{lj})] + [\hat{G}_{jl}^Q(\hat{Q}^l \mathbf{n}_{lj})]\nabla_j\}$$
$$+ \frac{3i}{ck_0}\{\nabla_j[\mathbf{q}_{jl} \times (\hat{M}^l \mathbf{n}_{lj})] + [\mathbf{q}_{jl} \times (\hat{M}^l \mathbf{n}_{lj})]\nabla_j\} \Big\},$$

$$\hat{M}^j = \frac{\hat{\alpha}_M}{2}[\nabla \mathbf{H}_0(\mathbf{r}_j) + \mathbf{H}_0(\mathbf{r}_j)\nabla]$$
$$+ \frac{\hat{\alpha}_M k_0^2}{2} \sum_{l \neq j}^N \left\{ \frac{c}{ik_0}(\nabla_j[\mathbf{g}_{jl} \times \mathbf{p}^l] + [\mathbf{g}_{jl} \times \mathbf{p}^l]\nabla_j) \right.$$
$$+ \varepsilon_S[\nabla_j(\hat{G}_{jl}^p \mathbf{m}^l) + (\hat{G}_{jl}^p \mathbf{m}^l)\nabla_j]$$
$$+ \frac{c}{ik_0}\{\nabla_j[\mathbf{q}_{jl} \times (\hat{Q}^l \mathbf{n}_{lj})] + [\mathbf{q}_{jl} \times (\hat{Q}^l \mathbf{n}_{lj})]\nabla_j\}$$
$$+ 3\varepsilon_S \left\{ \nabla_j[\hat{G}_{jl}^Q(\hat{M}^l \mathbf{n}_{lj})] + [\hat{G}_{jl}^Q(\hat{M}^l \mathbf{n}_{lj})]\nabla_j \right\} \Big\}, \tag{25}$$

where $j = 1, 2, 3, \ldots, N$, and ∇_j is the nabla operator with respect to $\mathbf{r}_j$.

Note that the cases of the rectangular periodic nanoparticle array with only ED, MD, or EQ response are considered in earlier works [10,37]. After solving the system (25) for an array of N nanoparticles, one can calculate the extinction power P_{ext}, using its multipole presentation [10,37,47],

$$P_{\text{ext}} = \frac{\omega}{2}\text{Im}\sum_{j=1}^N \left[\mathbf{E}_0^*(\mathbf{r}_j) \cdot \mathbf{p}^j + \mu_0 \frac{[\nabla \mathbf{H}_0^*(\mathbf{r}_j)]^T}{2} : \hat{M}^j \right.$$
$$\left. + \mu_0 \mathbf{H}_0^*(\mathbf{r}_j) \cdot \mathbf{m}^j + \frac{\nabla \mathbf{E}_0^*(\mathbf{r}_j) + \mathbf{E}_0^*(\mathbf{r}_j)\nabla}{12} : \hat{Q}^j \right], \tag{26}$$

where the asterisk $*$ denotes complex conjugation, T denotes the transpose operation, and the signs $\cdot$ and $:$ denote the scalar products between vectors and dyads (tensors), respectively [17].

B. Dipole and quadrupole polarizabilities of a sphere

Let us consider homogeneous nanoparticles of spherical shape. In this case, the multipole responses of the nanoparticles are characterized by corresponding *scalar* polarizabilities α_p, α_m, α_Q, and α_M for ED, MD, EQ, and MQ, respectively. In this subsection, we demonstrate the approach to derive effective polarizabilities of spherical particles through Mie coefficients. We show it based on the example of the MQ, and we refer to the literature (see, e.g., [10,37]) for derivations and expressions of ED, MD, and EQ.

For a single nanoparticle located at the origin of a coordinate system, the angular dependence of the complex scattered electric fields E_θ and E_ϕ in the far-field can be written as [48]

$$E_\theta \approx E_0 \frac{e^{ik_S r}}{-ik_S r} \cos\phi \sum_{n=1}^\infty \frac{2n+1}{n(n+1)}\left(a_n \frac{dP_n^1}{d\theta} + b_n \frac{P_n^1}{\sin\theta} \right),$$

$$E_\phi \approx -E_0 \frac{e^{ik_S r}}{-ik_S r} \sin\phi \sum_{n=1}^\infty \frac{2n+1}{n(n+1)}\left(a_n \frac{P_n^1}{\sin\theta} + b_n \frac{dP_n^1}{d\theta} \right),$$
$$\tag{27}$$

where E_0 is the strength (amplitude) of the incident electric field, θ and ϕ are the polar and azimuth scattering angles, respectively, n defines the degree of the multipole mode, i.e., $n = 1$ and 2 for dipole and quadrupole modes, respectively, P_n^1 represents the set of associated Legendre polynomials of order 1, $P_2^1(\cos\theta) = 3\cos\theta\sin\theta$, $dP_2^1/d\theta = 3(\cos^2\theta - \sin^2\theta)$, and a_n and b_n are the complex Mie coefficients calculated by evaluating the overlap integral between the incident field and the field associated with the natural modes of the system. For MQ related to the coefficient b_2,

$$E_\theta^M \approx E_0 \frac{e^{ik_S r}}{-ik_S r}\cos\phi\frac{5}{2}b_2\cos\theta,$$

$$E_\phi^M \approx -E_0 \frac{e^{ik_S r}}{-ik_S r}\sin\phi\frac{5}{2}b_2(-\sin^2\theta + \cos^2\theta). \quad (28)$$

From another side, the angular field components can be expressed as [47]

$$E_\theta^M(r,\phi,\theta) = \frac{-ik_S}{2}\sqrt{\frac{\mu_0}{\varepsilon_0\varepsilon_S}}\frac{k_S^2 e^{ik_S r}}{4\pi r}(\mu_y\cos\phi - \mu_x\sin\phi),$$

$$E_\phi^M(r,\phi,\theta) = \frac{-ik_S}{2}\sqrt{\frac{\mu_0}{\varepsilon_0\varepsilon_S}}\frac{k_S^2 e^{ik_S r}}{4\pi r}(-\mu_x\cos\phi\cos\theta$$
$$-\mu_y\sin\phi\cos\theta + \mu_z\sin\theta), \quad (29)$$

where the vector $\mu \equiv (\hat{M}\mathbf{n})$ and for the sphere $\mu = (0, n_z, n_y)M_0 = (0, \cos\theta, \sin\theta\sin\phi)M_0$. Here we consider that the nanoparticle is illuminated by a monochromatic plane wave with linear polarization along the x-axis similar to the case from [37]. Taking into account that the incident magnetic field $\mathbf{H} = (0, H_0, 0)\exp(ik_S z)$ and $\hat{M} = \alpha_M(\nabla\mathbf{H} + \mathbf{H}\nabla)/2$, one obtains $M_0 = M_{yz} = M_{zy} = \alpha_M(ik_S/2)H_0 = \alpha_M(ik_S/2)\sqrt{\varepsilon_0\varepsilon_S/\mu_0}E_0$. Then, comparing (28) and (29), we obtain an expression for MQ polarizability:

$$\alpha_M = i\frac{40\pi}{k_S^5}b_2. \quad (30)$$

The other three polarizabilities of interest—α_p, α_m, and α_Q—are expressed through the scattering coefficients a_1, b_1, and a_2 of Mie theory as (see, e.g., [49])

$$\alpha_p = i\frac{6\pi\varepsilon_0\varepsilon_S}{k_S^3}a_1, \quad \alpha_m = i\frac{6\pi}{k_S^3}b_1, \quad \alpha_Q = i\frac{120\pi\varepsilon_0\varepsilon_S}{k_S^5}a_2. \quad (31)$$

In Mie theory, contributions of all toroidal moments are included in the scattering coefficients a_j and b_j. Therefore, our theoretical model automatically takes into account the toroidal moments associated with the considered coefficients a_1, b_1, a_2, and b_2. In particular, the coefficient a_1 includes a contribution of the toroidal dipole moment.

C. Infinite periodic array of identical spheres

1. Effective polarizabilities of a sphere in an array

Previous works [10,37] have shown that in the infinite periodic two-dimensional array with a single nanoparticle in the elementary cell, ED does not couple to either EQ [37] or MD [10], and all nanoparticles of the array have the same induced ED, MD, and EQ moments at the normal incidence of
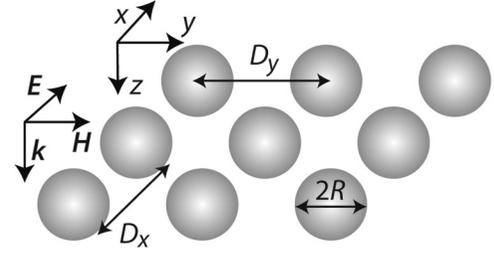

FIG. 1. Schematic of the rectangular periodic nanoparticle array under consideration.

external light excitation. We have also shown that the coupling of EQ and MD takes place in the infinite arrays [40]. In the present work, we generalize the concept to four multipoles ED, MD, EQ, and MQ and demonstrate the coupling of ED and MQ.

Let us consider a normally incident, monochromatic, and x-polarized light wave with field components $(E_x(\mathbf{r}) = E_0\exp(ik_S z), H_y(\mathbf{r}) = H_0\exp(ik_S z), 0)$ (Fig. 1). Under these conditions, the dipole and quadrupole moments of the identical spherical nanoparticles in infinite periodic rectangular arrays will be the same for all nanoparticles and have the following components: $\mathbf{p} = (p_0\hat{x} + 0\hat{y} + 0\hat{z})$, $\mathbf{m} = (0\hat{x} + m_0\hat{y} + 0\hat{z})$, $\hat{Q} = Q_0(\hat{x}\hat{z} + \hat{z}\hat{x})$, and $\hat{M} = M_0(\hat{y}\hat{z} + \hat{z}\hat{y})$, where $\hat{x}$, $\hat{y}$, and $\hat{z}$ are the unit vectors of the Cartesian coordinate system. In this case, the general system of Eqs. (25) can be simplified to the following form:

$$p_0 = \alpha_p E_x(\mathbf{r}_0) + \frac{\alpha_p}{\varepsilon_0}\left[S_{pp}p_0 + \frac{ik_0}{c}S_{pM}M_0\right],$$

$$m_0 = \alpha_m H_y(\mathbf{r}_0) + \alpha_m\left[S_{mm}m_0 + \frac{ck_0}{i}S_{mQ}Q_0\right],$$

$$Q_0 = \frac{\alpha_Q ik_S E_x(\mathbf{r}_0)}{2} + \frac{\alpha_Q}{2\varepsilon_0}\left[\frac{ik_0}{c}S_{Qm}m_0 + S_{QQ}Q_0\right],$$

$$M_0 = \frac{\alpha_M ik_S H_y(\mathbf{r}_0)}{2} + \frac{\alpha_M}{2}\left[\frac{ck_0}{i}S_{Mp}p_0 + S_{MM}M_0\right], \quad (32)$$

where $\mathbf{r}_0$ is the position of an arbitrary particle with the number 0 in the array, and we will consider that this particle is located at the origin of the chosen Cartesian coordinate system (Fig. 1) throughout the work. The multipole sums in (32) are

$$S_{pp} \equiv k_0^2\sum_{l\neq 0}G_{xx}^p(0,\mathbf{r}_l) = \frac{k_0^2}{4\pi}\sum_{l\neq 0}\frac{e^{ik_S r_l}}{r_l}\left(1 + \frac{i}{k_S r_l}\right.$$
$$\left. - \frac{1}{k_S^2 r_l^2} - \frac{x_l^2}{r_l^2} - \frac{i3x_l^2}{k_S r_l^3} + \frac{3x_l^2}{k_S^2 r_l^4}\right), \quad (33)$$

$$S_{mm} \equiv k_S^2\sum_{l\neq 0}G_{yy}^p(0,\mathbf{r}_l) = \frac{k_S^2}{4\pi}\sum_{l\neq 0}\frac{e^{ik_S r_l}}{r_l}\left(1 + \frac{i}{k_S r_l}\right.$$
$$\left. - \frac{1}{k_S^2 r_l^2} - \frac{y_l^2}{r_l^2} - \frac{i3y_l^2}{k_S r_l^3} + \frac{3y_l^2}{k_S^2 r_l^4}\right), \quad (34)$$

$$S_{QQ} = \frac{k_0^2}{6} \frac{ik_S}{4\pi} \sum_{l \neq 0} \frac{e^{ik_S r_l}}{r_l^2} \left(-2 - i\frac{6 + k_S^2 x_l^2}{k_S r_l} + \frac{12 + 7k_S^2 x_l^2}{k_S^2 r_l^2} \right.$$
$$\left. + i\frac{12 + 27k_S^2 x_l^2}{k_S^3 r_l^3} - \frac{60x_l^2}{k_S^2 r_l^4} - \frac{i60x_l^2}{k_S^3 r_l^5} \right), \qquad (35)$$

$$S_{MM} = \frac{k_0^2 \varepsilon_S}{2} \frac{ik_S}{4\pi} \sum_{l \neq 0} \frac{e^{ik_S r_l}}{r_l^2} \left(-2 - i\frac{6 + k_S^2 y_l^2}{k_S r_l} + \frac{12 + 7k_S^2 y_l^2}{k_S^2 r_l^2} \right.$$
$$\left. + i\frac{12 + 27k_S^2 y_l^2}{k_S^3 r_l^3} - \frac{60y_l^2}{k_S^2 r_l^4} - \frac{i60y_l^2}{k_S^3 r_l^5} \right), \qquad (36)$$

$$S_{mQ} \equiv \frac{1}{Q_0} \sum_{l \neq 0} [\mathbf{q}_{0l} \times (\hat{Q}^l \mathbf{n}_{l0})]_y$$
$$= \frac{1}{6} \frac{k_S^2}{4\pi} \sum_{l \neq 0} \frac{x_l^2 e^{ik_S r_l}}{r_l^3} \left(-1 - \frac{3i}{k_S r_l} + \frac{3}{k_S^2 r_l^2} \right), \qquad (37)$$

$$S_{Qm} \equiv \frac{1}{m_0} \sum_{l \neq 0} [\nabla_0[\mathbf{g}_{0l} \times \mathbf{m}^l] + [\mathbf{g}_{0l} \times \mathbf{m}^l]\nabla_0]_{xz}$$
$$= 6S_{mQ} = \frac{k_S^2}{4\pi} \sum_{l \neq 0} \frac{x_l^2 e^{ik_S r_l}}{r_l^3} \left(-1 - \frac{3i}{k_S r_l} + \frac{3}{k_S^2 r_l^2} \right), \quad (38)$$

$$S_{pM} \equiv \frac{1}{M_0} \sum_{l \neq 0} [\mathbf{q}_{0l} \times (\hat{M}^l \mathbf{n}_{l0})]_x$$
$$= \frac{-k_S^2}{8\pi} \sum_{l \neq 0} \frac{y_l^2 e^{ik_S r_l}}{r_l^3} \left(-1 - \frac{3i}{k_S r_l} + \frac{3}{k_S^2 r_l^2} \right), \qquad (39)$$

$$S_{Mp} \equiv \frac{1}{p_0} \sum_{l \neq 0} [\nabla_0[\mathbf{g}_{0l} \times \mathbf{p}^l] + [\mathbf{g}_{0l} \times \mathbf{p}^l]\nabla_0]_{yz} = 2S_{pM}$$
$$= \frac{-k_S^2}{4\pi} \sum_{l \neq 0} \frac{y_l^2 e^{ik_S r_l}}{r_l^3} \left(-1 - \frac{3i}{k_S r_l} + \frac{3}{k_S^2 r_l^2} \right). \qquad (40)$$

If we do not take into account the terms proportional to S_{pM}, S_{mQ}, S_{Qm}, S_{Mp} corresponding to the cross-multipole coupling in the system Eqs. (32), the effective polarizabilities of dipoles and quadrupoles without coupling to other multipoles are obtained as [10,37]

$$\frac{1}{\alpha_p^{\text{eff}}} = \frac{1}{\alpha_p} - \frac{S_{pp}}{\varepsilon_0}, \quad \frac{1}{\alpha_m^{\text{eff}}} = \frac{1}{\alpha_m} - S_{mm},$$
$$\frac{1}{\alpha_Q^{\text{eff}}} = \frac{1}{\alpha_Q} - \frac{S_{QQ}}{2\varepsilon_0}, \quad \frac{1}{\alpha_M^{\text{eff}}} = \frac{1}{\alpha_M} - \frac{S_{MM}}{2}. \qquad (41)$$

However, in the system (32), the coefficients S_{mQ}, S_{Qm}, S_{pM}, and S_{Mp} are not equal to 0 for infinite arrays providing coupling between MD and EQ moments as well as between ED and MQ moments. By solving the whole system (32) taking into account the cross-multipole coupling, one can find the total effective polarizabilities of the particles in the array. These polarizabilities are determined by the expressions $\alpha_p^{\text{eff/coup}} = p_0/E_x$, $\alpha_m^{\text{eff/coup}} = m_0/H_y$, $\alpha_Q^{\text{eff/coup}} =$

$2Q_0/(ik_S E_x)$, and $\alpha_M^{\text{eff/coup}} = 2M_0/(ik_S H_y)$ taking into account $H_y = E_x\sqrt{\varepsilon_S \varepsilon_0/\mu_0}$.

Thus we obtain

$$\frac{1}{\alpha_p^{\text{eff/coup}}} = \frac{1 - S_{Mp}\alpha_p^{\text{eff}} S_{pM}\alpha_M^{\text{eff}} k_0^2/(2\varepsilon_0)}{\alpha_p^{\text{eff}}[1 - S_{pM}\alpha_M^{\text{eff}} k_S^2/2]}, \qquad (42)$$

$$\frac{1}{\alpha_m^{\text{eff/coup}}} = \frac{1 - S_{Qm}\alpha_m^{\text{eff}} S_{mQ}\alpha_Q^{\text{eff}} k_0^2/(2\varepsilon_0)}{\alpha_m^{\text{eff}}[1 + S_{mQ}\alpha_Q^{\text{eff}} k_0^2/(2\varepsilon_0)]}, \qquad (43)$$

$$\frac{1}{\alpha_Q^{\text{eff/coup}}} = \frac{1 - S_{Qm}\alpha_m^{\text{eff}} S_{mQ}\alpha_Q^{\text{eff}} k_0^2/(2\varepsilon_0)}{\alpha_Q^{\text{eff}}[1 + S_{Qm}\alpha_m^{\text{eff}}]}, \qquad (44)$$

$$\frac{1}{\alpha_M^{\text{eff/coup}}} = \frac{1 - S_{Mp}\alpha_p^{\text{eff}} S_{pM}\alpha_M^{\text{eff}} k_0^2/(2\varepsilon_0)}{\alpha_M^{\text{eff}}[1 - S_{Mp}\alpha_p^{\text{eff}}/(\varepsilon_0 \varepsilon_S)]}. \qquad (45)$$

The presentations (42)–(45) of the polarizabilities allow for analysis of the roles of coupling effects in nanoparticle arrays.

2. Conditions of lattice resonances and polarizability suppression due to cross-multipole coupling

General expressions (42)–(45) demonstrate that, due to the cross-multipole coupling, the ED and MQ lattice resonances are excited at the conditions

$$\left[\frac{1}{\alpha_p^{\text{eff}}\alpha_M^{\text{eff}}} - \frac{S_{Mp}S_{pM}k_0^2}{2\varepsilon_0} \right] \to 0. \qquad (46)$$

The similar conditions of the MD and EQ lattice resonances can be written out from (43) and (44), respectively.

Let us analyze the condition when the effective MQ polarizability of the nanoparticle in the periodic lattice vanishes and the nanoparticles do not have considerable MQ response. From Eq. (45), one can see that $\alpha_M^{\text{eff/coup}} = 0$ occurs at the condition $1/\alpha_p^{\text{eff}} - S_{Mp}/(\varepsilon_0 \varepsilon_S) = 0$, which means

$$\text{Re}\left[\frac{1}{\alpha_p^{\text{eff}}} \right] = \text{Re}\left[\frac{S_{Mp}}{\varepsilon_0 \varepsilon_S} \right] \quad \text{and} \quad \text{Im}\left[\frac{1}{\alpha_p^{\text{eff}}} \right] = \text{Im}\left[\frac{S_{Mp}}{\varepsilon_0 \varepsilon_S} \right]. \qquad (47)$$

This condition is similar to the condition for conventional lattice resonances in the array of identical multipoles, e.g., from Eqs. (41), electric dipoles with $\text{Re}[1/\alpha_p] = \text{Re}[S_{pp}]/\varepsilon_0$ or electric quadrupoles $\text{Re}[1/\alpha_Q] = \text{Re}[S_{QQ}]/(2\varepsilon_0)$ [10,37]. As we show below, the condition for imaginary parts in (47) can be satisfied approximately. The imaginary part of the lattice sum can only affect the radiative losses in the system. In contrast, the imaginary part of the inverse multipole polarizability contains, in general, two contributions that correspond to absorptive and radiative losses. Discussion of this issue with respect to the dipole systems can be found, for example, in Ref. [50]. Surprisingly, the spectral position of $\alpha_M^{\text{eff/coup}} = 0$ does not depend on the $\alpha_M^{\text{eff/coup}}$ values and is defined solely by the values in Eq. (47), which are α_p and lattice parameters.

One can also derive from Eq. (42) that under the condition of Eq. (47),

$$\frac{1}{\alpha_p^{\text{eff/coup}}} = \frac{1}{\alpha_p^{\text{eff}}}, \quad (48)$$

which means that the excitation of MQ moments is suppressed in the array with the parameters satisfying the condition (47) because of the dipole-quadrupole coupling.

Similar to the case of MQ, one can derive a condition of vanishing ED because of cross-multipole coupling in the periodic lattice. From Eq. (42), one can see that $\alpha_p^{\text{eff/coup}} = 0$ occurs at the condition $1 - S_{pM}\alpha_M^{\text{eff}}k_S^2/2 = 0$, which effectively means

$$\frac{1}{\alpha_M^{\text{eff/coup}}} = \frac{1}{\alpha_M^{\text{eff}}} = \frac{S_{pM}k_S^2}{2}. \quad (49)$$

Again the condition (49) can be satisfied only approximately for the imaginary part. Similar to Eqs. (47)–(49), the analysis can be done for MD and EQ polarizabilities.

3. Reflection and transmission coefficients

After calculations of the effective polarizabilities of the nanoparticles in an array, using Eqs. (42)–(45), the reflection and transmission coefficients can be obtained if we consider the total electric field in the far-field region for $z < 0$ and $z > 0$:

$$\mathbf{E} = \mathbf{E}_0 + \mathbf{E}_p + \mathbf{E}_m + \mathbf{E}_Q + \mathbf{E}_M. \quad (50)$$

The total electric field is a superposition of the incident field $\mathbf{E}_0$ and the fields generated by the nanoparticle multipole moments. For x-polarization of the incident wave, the electric fields generated by ED, MD, EQ, and MQ of nanoparticles are

$$\mathbf{E}_p = \frac{k_0^2}{\varepsilon_0}E_x\alpha_p^{\text{eff/coup}}\left(G_{xx}^r, 0, 0\right), \quad (51)$$

$$\mathbf{E}_m = -\frac{ik_0}{c\varepsilon_0}H_y\alpha_m^{\text{eff/coup}}\left(g_z^r, 0, 0\right), \quad (52)$$

$$\mathbf{E}_Q = \frac{k_0^2}{\varepsilon_0}\frac{ik_S E_x}{2}\alpha_Q^{\text{eff/coup}}\left(G_x^{Q,r}, 0, 0\right), \quad (53)$$

$$\mathbf{E}_M = -\frac{ik_0}{2c\varepsilon_0}\frac{ik_S H_y}{2}\alpha_M^{\text{eff/coup}}\left(G_x^{M,r}, 0, 0\right), \quad (54)$$

respectively. Here, E_x and $H_y = \sqrt{\varepsilon_0\varepsilon_S/\mu_0}E_x$ are the electric- and magnetic-field amplitudes of the incident wave. Finally, from (50) the nonzero total electric-field component E_x^f in the far-field approximation is

$$E_x^f = E_x\left[e^{ik_Sz} + \frac{k_0^2}{\varepsilon_0}\alpha_p^{\text{eff/coup}}G_{xx}^r - ik_S\alpha_m^{\text{eff/coup}}g_z^r \right.$$
$$\left. + \frac{k_0^2}{\varepsilon_0}\alpha_Q^{\text{eff/coup}}\frac{ik_S}{2}G_x^{Q,r} + \frac{k_S^2}{4}\alpha_M^{\text{eff/coup}}G_x^{M,r}\right], \quad (55)$$

where the far-field approximation of the Green's tensor components, taking into account the lattice and that the

wavelengths are larger than the array periods, is

$$G_{xx}^r = \sum_{j=1}^{\infty}\left[1 + \frac{1}{k_S^2}\frac{\partial^2}{\partial x^2}\right]\Phi(\mathbf{r}, \mathbf{r}_j) \approx \frac{i}{2S_L k_S}e^{\mp ik_Sz}, \quad (56)$$

$$g_z^r = \sum_{j=1}^{\infty}\frac{\partial}{\partial z}\Phi(\mathbf{r}, \mathbf{r}_j) \approx \pm\frac{1}{2S_L}e^{\mp ik_Sz} \quad (57)$$

for ED and MD terms, respectively, and

$$G_x^{Q,r} = \sum_{j=1}^{\infty}\left[-\frac{1}{6}\frac{\partial}{\partial z} - \frac{1}{3k_S^2}\frac{\partial^3}{\partial x^2\partial z}\right]\Phi(\mathbf{r}, \mathbf{r}_j) \approx \mp\frac{e^{\mp ik_Sz}}{12S_L}, \quad (58)$$

$$G_x^{M,r} = \sum_{j=1}^{\infty}\left[\frac{\partial^2}{\partial y^2} - \frac{\partial^2}{\partial z^2}\right]\Phi(\mathbf{r}, \mathbf{r}_j) \approx \frac{ik_S}{2S_L}e^{\mp ik_Sz} \quad (59)$$

for EQ and MQ terms, respectively. Here

$$\Phi(\mathbf{r}, \mathbf{r}_j) = \frac{e^{ik_S|\mathbf{r}-\mathbf{r}_j|}}{4\pi|\mathbf{r}-\mathbf{r}_j|} \quad (60)$$

is the scalar Green's function of homogeneous medium with ε_S, S_L is the area of the lattice unit cell, and the upper sign corresponds to $z < 0$ and the lower sign for the case when $z > 0$. Calculations of the sums in (56)–(59) are carried out by the method shown in Ref. [10] and account for all particles in the array.

In this approach, the reflection and transmission coefficients, both with respect to electric field, are (compare with [10])

$$r_0 = \frac{ik_S}{2S_L}\left[\frac{1}{\varepsilon_0\varepsilon_S}\alpha_p^{\text{eff/coup}} - \alpha_m^{\text{eff/coup}} - \frac{k_0^2}{12\varepsilon_0}\alpha_Q^{\text{eff/coup}} \right.$$
$$\left. + \frac{k_S^2}{4}\alpha_M^{\text{eff/coup}}\right], \quad (61)$$

$$t_0 = 1 + \frac{ik_S}{2S_L}\left[\frac{1}{\varepsilon_0\varepsilon_S}\alpha_p^{\text{eff/coup}} + \alpha_m^{\text{eff/coup}} + \frac{k_0^2}{12\varepsilon_0}\alpha_Q^{\text{eff/coup}} \right.$$
$$\left. + \frac{k_S^2}{4}\alpha_M^{\text{eff/coup}}\right]. \quad (62)$$

Note that the expressions of (61) and (62) can be obtained from the formulas of the reflection and transmission coefficients presented in [51], for x-polarization, if one writes the multipole moments of spherical nanoparticles through the corresponding polarizabilities.

The intensity reflection R_0 and transmission T_0 coefficients are

$$R_0 = |r_0|^2, \quad T_0 = |t_0|^2.$$

Note that the expressions (61) and (62) are obtained for the case when the wavelength of the incident light is larger than the periods of the array. However, these expressions can also be applied to calculate the transmission and reflection coefficients of zero diffraction order in nanoparticle arrays with an arbitrary relation between the wavelength of the incident light and array periods.
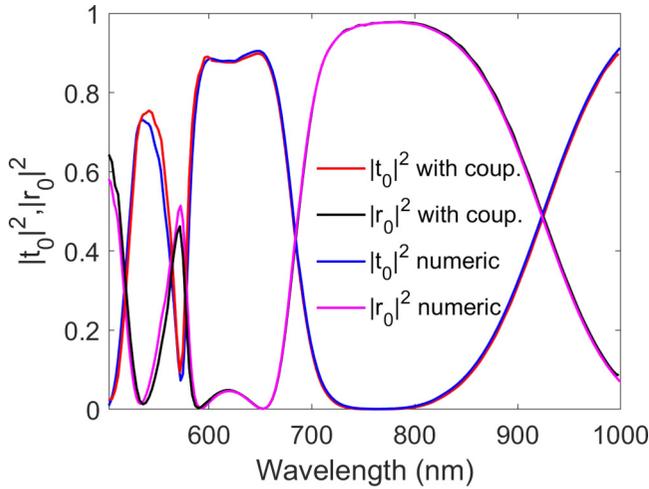
FIG. 2. Analytical (denoted "with coup.") and numerical calculations (denoted "numeric") of the intensity reflection and transmission coefficients for the infinite periodic array of silicon spheres. The lattice periods are $D_x = D_y = 300$ nm, and the silicon particles have radius $R = 125$ nm.

IV. APPLICATIONS

To demonstrate the applicability of the developed approach, in this section we perform analytical calculations following the equations derived above and numerical simulations using the frequency-domain solver in CST Microwave Studio. Crystalline silicon spheres with $R = 125$ nm are considered, ensuring that strong dipole and quadrupole resonances are excited in the visible and near-infrared spectral range. Crystalline silicon permittivity is taken from the experimental data [52] and illustrated elsewhere [10]. In our simulations, the surrounding material has dielectric permittivity $\varepsilon_S = 1$ and the normally incident light is polarized along the x-axis (see Fig. 1).

To start with, we perform analytical calculations of reflection and transmission for a square array with periods $D_x = D_y = 300$ nm using Eqs. (61) and (62). The comparison of these calculations with the results of numerical simulations are shown in Fig. 2. There is a good agreement confirming that the multipole model derived above can be successfully applied to predict optical properties of high-density arrays. Moreover, the polarizability presentations (61) and (62) allow us to study the coupling effects in detail.

A. Multipole coupling

Let us analyze the influence of a nanoparticle lattice on multipole effective polarizabilities. As is expected, the pronounced effect is realized at the resonant conditions. Figure 3 shows the spectral behavior of ED and MQ polarizabilities [panel (a)] and MD and EQ polarizabilities [panel (b)] for three cases under consideration. The first case is a single sphere, and calculations are performed with Eqs. (30) and (31) (solid lines in Fig. 3). The second case is a sphere in the lattice without cross-multipole coupling. Effectively, this case corresponds to the lattice of the same multipoles, and calculations are performed with Eqs. (41) (dashed lines in Fig. 3).
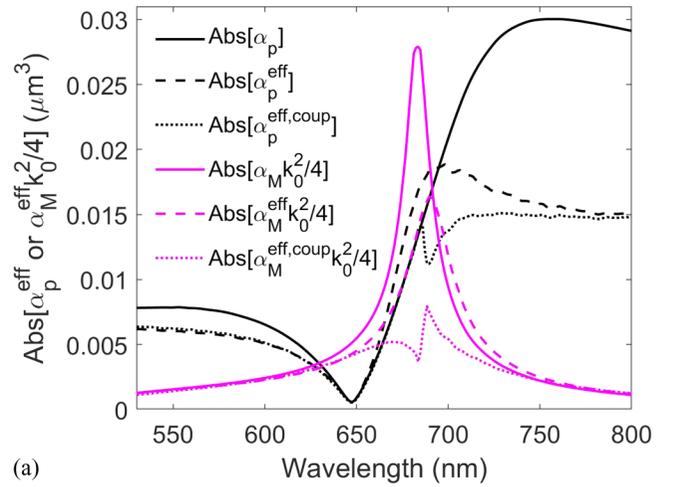
(a)
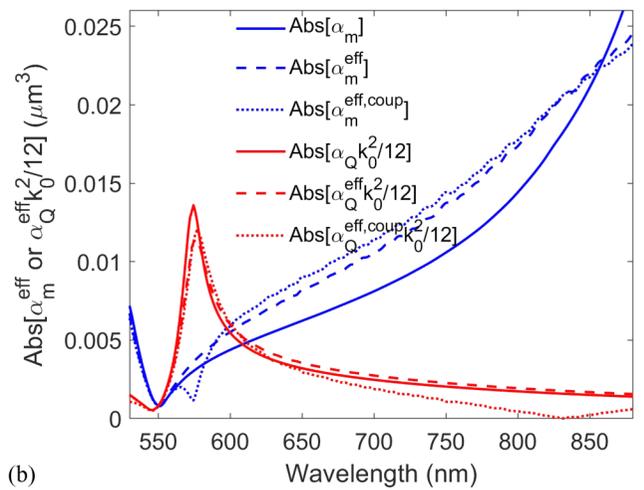
(b)

FIG. 3. Multipole resonances in the individual sphere and its periodic array. The lattice periods are $D_x = D_y = 300$ nm, and silicon particles have $R = 125$ nm. Absolute values of (a) ED and MQ and (b) MD and EQ multipole effective polarizabilities. The effective polarizabilities are calculated with Eqs. (30) and (31) for the single sphere, Eqs. (41) for the sphere in the array without cross-multipole coupling, and Eqs. (42)–(45) taking into account coupling. Effective polarizabilities of MQ and EQ are normalized to $k_0^2/4$ and $k_0^2/12$, respectively, following the coefficients in Eqs. (61) and (62), and all electric dipole and quadrupole polarizabilities are divided on ε_0.

Finally, the third case is a sphere in the lattice, and coupling of all the multipoles is taken into account with Eqs. (42)–(45) (dotted lines in Fig. 3). While the polarizabilities of the single sphere differ from the polarizabilities of the spheres in the array, calculations taking and not taking into account cross-multipole coupling are very similar in a wide range of the spectrum. However, in proximity to resonances, the coupling is strong and significantly changes the effective polarizability of the particle. In particular, the value of $|\alpha_M^{\mathrm{eff,coup}} k_0^2/4|$ is significantly suppressed at the resonant region due to energy exchange between MQ and ED [$\lambda \approx 680$ nm, Fig. 3(a)]. Moreover, due to the coupling, the resonances of ED and MQ polarizabilities demonstrate Fano-type profiles, where the maximum of the MQ term coincides with the minimum of the ED term and vice versa [$\lambda \approx 680$ nm, Fig. 3(a)]. Similar
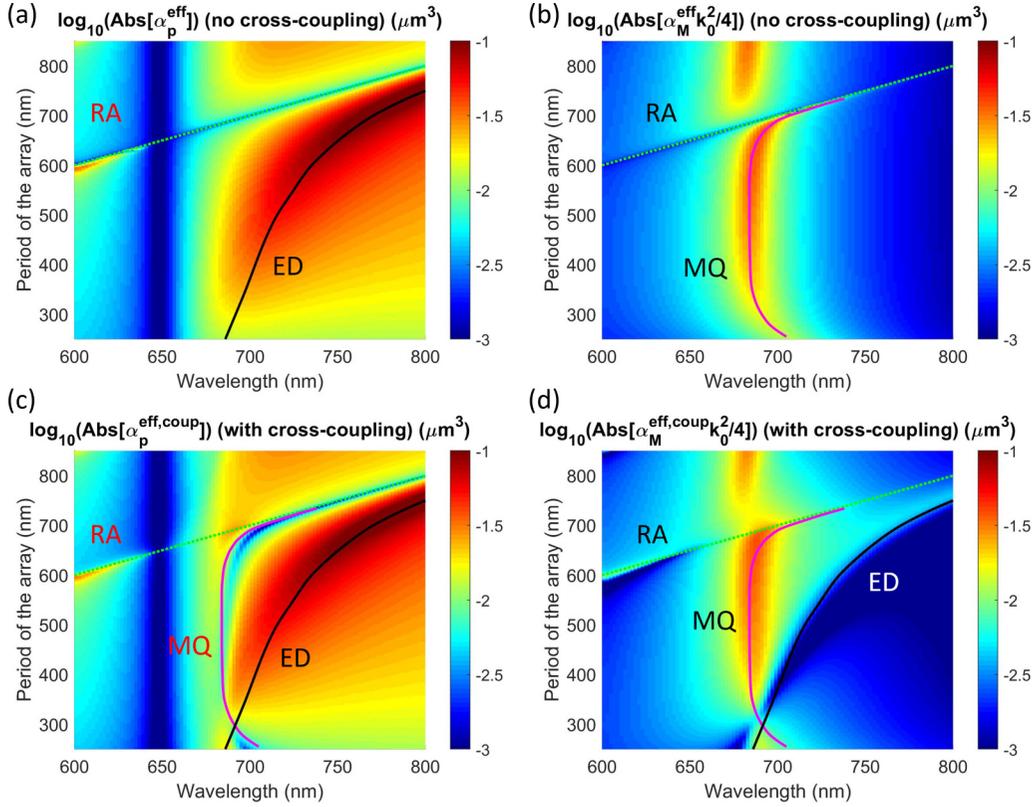
FIG. 4. Effective polarizabilities of (a),(c) ED and (b),(d) MQ. Panels (a) and (b) were calculated without accounting for cross-multipole coupling between ED and MQ, and panels (c) and (d) were calculated with the cross-multipole coupling. The lattice periods are $D_x = D_y$, and silicon particles have $R = 125$ nm. The results are shown in a logarithmic scale. Note that the plotted quantity is $\log_{10}$ of the absolute value of the effective multipole polarizability and takes into account $k_0^2/4$ for MQ. The dotted lines labeled RA mark the position of Rayleigh anomaly. Here all electric dipole and quadrupole polarizabilities are divided on ε_0.

behavior can be observed for another MD-EQ multipole pair: the MD term $|\alpha_m^{\mathrm{eff,coup}}|$ experiences a decrease at the same wavelength that the EQ term $|\alpha_Q^{\mathrm{eff}}k_0^2/12|$ has a peak ($\lambda \approx 575$ nm), and the EQ term $|\alpha_Q^{\mathrm{eff,coup}}k_0^2/12|$ has a near-zero value in proximity to the MD term $|\alpha_m^{\mathrm{eff}}|$ peak [$\lambda \approx 825$ nm, Fig. 3(b)]. Thus, the cross-multipole coupling in the arrays may cause significant changes (especially at the resonant conditions)

and needs to be taken into account in the array multipole approximations.

To demonstrate the role of the array periodicity in the cross-multipole coupling effects, we calculated the ED and MQ polarizabilities without and with the cross-multipole coupling term as a function of the array period and incident light wavelength. Results are shown in Fig. 4. Without cross-multipole coupling, panels (a) and (b) include only the ED
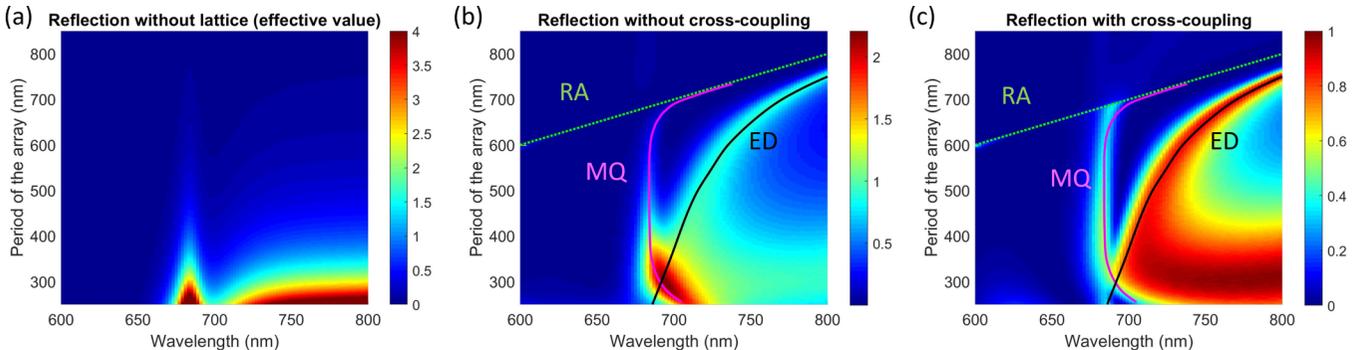

FIG. 5. Intensity reflection coefficient from the array of particles with the lattice periods $D_x = D_y$ and silicon particles $R = 125$ nm. (a) Calculations are performed using only single-particle polarizability Eqs. (31), without taking into account the interaction of particles in the lattice. (b) Calculations are performed with polarizabilities defined through Eqs. (41) and accounting only for the interactions of multipoles of the same kind in the lattice. (c) Calculations with cross-multipole coupling of the multipoles defined by Eqs. (42)–(45). Panels (a) and (b) include regions with unphysical results with the reflection coefficient values greater than 1. The dotted lines labeled RA mark the position of the Rayleigh anomaly.

and MQ resonances, respectively, which are affected only by the Rayleigh anomaly (RA lines in Fig. 4). In contrast, in the case of the cross-multipole coupling, panels (c) and (d) also demonstrate the antiresonant regions, where ED polarizability is suppressed in proximity to MQ resonances [panel (c)] and vice versa [panel (d)]. Note that, at a period of 300 nm, both ED and MQ polarizabilities are suppressed due to the cross-multipole coupling effect.

In experimental investigations, it is not possible to obtain direct information about nanoparticle polarizability in the arrays. Therefore, it is important to understand how the cross-multipole coupling effects can appear in reflection and transmission. So we calculate the reflection from the array in all the cases under consideration: (i) polarizability of the single particle (without account of the array), (ii) coupling of the multipoles of the same kind in the lattice, and (iii) cross-multipole coupling (Fig. 5). Without multipole coupling, the reflection coefficient is significantly overestimated in the resonant regions and has unphysical values larger than unit [panels (a) and (b)]. In contrast to the case without cross-multipole coupling, the reflection coefficient calculated with the cross-multipole coupling polarizabilities [Fig. 5(c)] does not contradict the physical requirement that $R_0 + T_0 \leqslant 1$, which results from energy conservation for passive systems.

B. Demonstration of polarizability suppression

As has been shown above, the effective polarizability of ED and MQ can be significantly reduced down to near-zero value if the conditions (47)–(49) are satisfied, which can be typically achieved in proximity to the resonances. Here we verify these conditions. Figure 6(a) shows that upon overlap of ED and MQ resonances in the dense lattice with $D_x = D_y = 270$ nm, the ED and MQ polarizabilities experience a minimum.

We compare the corresponding cross-multipole coupling sum S_{pM} and S_{Mp} with inverse ED and MQ polarizabilities $1/\alpha_p^{\text{eff}}$ and $1/\alpha_M^{\text{eff}}$ shown in Figs. 6(b) and 6(c). The results confirm that the polarizability minimum in Fig. 6(a) happens at the spectral point where conditions defined by Eqs. (47) and (49) are exactly satisfied for the real parts of the sum and inverse polarizabilities,

$$\frac{\text{Re}(S_{Mp}/\varepsilon_0\varepsilon_S)}{\text{Re}(1/\alpha_p^{\text{eff}})} = 1 \quad \text{or} \quad \frac{\text{Re}(S_{pM}k_S^2/2)}{\text{Re}(1/\alpha_M^{\text{eff}})} = 1.$$

In turn, the conditions for imaginary parts are satisfied only approximately. In the case shown in Figs. 6(b) and 6(c), it is

$$\frac{\text{Im}(S_{Mp}/\varepsilon_0\varepsilon_S)}{\text{Im}(1/\alpha_p^{\text{eff}})} \approx 0.90 \quad \text{or} \quad \frac{\text{Im}(S_{pM}k_S^2/2)}{\text{Im}(1/\alpha_M^{\text{eff}})} \approx 0.86.$$

The near-zero EQ polarizability in the cross-multipole coupling model at the wavelength 825 nm in Fig. 3(b) also occurs due to the cross-multipole coupling between EQ and MD moments.

C. Lattice anapole effect

Recent work has shown [51] that light can be transmitted almost unperturbed by the lattices (metasurfaces) composed of dielectric nanoparticles supporting resonant optical response. This lattice invisibility effect is realized due to light
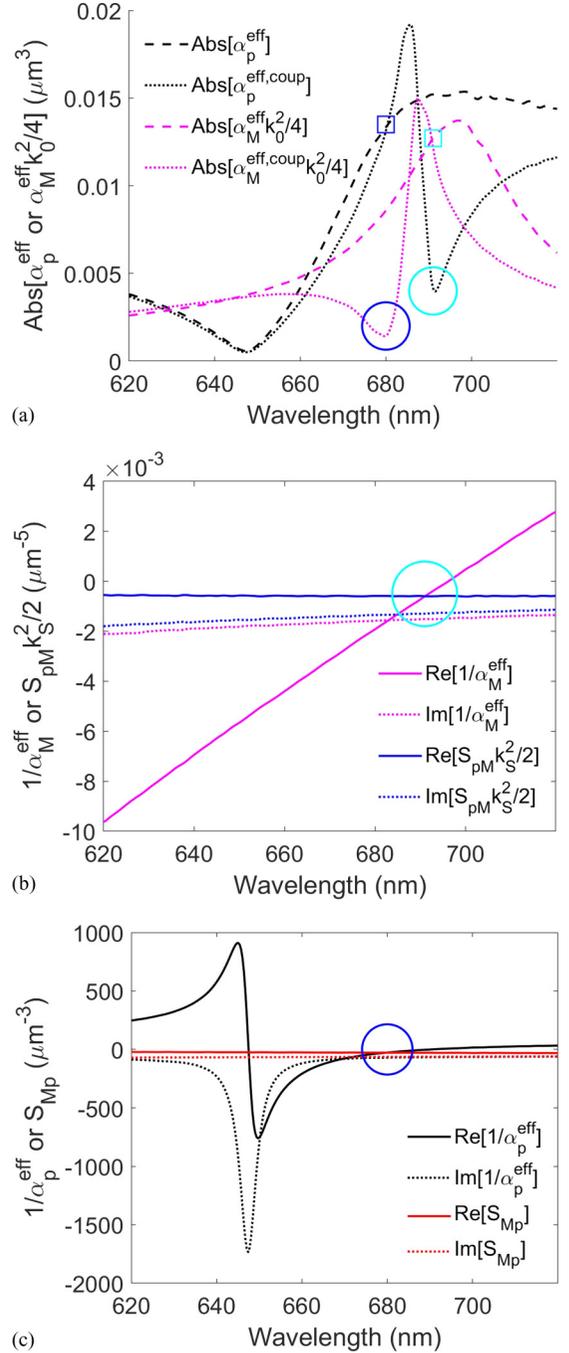

(a)

(b)

(c)

FIG. 6. Cross-multipole coupling of ED and MQ in the lattice. The lattice periods are $D_x = D_y = 270$ nm, and silicon particles have $R = 125$ nm. (a) Absolute values of ED and MQ effective polarizabilities without and with cross-multipole coupling. Effective polarizability of MQ is normalized to $k_0^2/4$ following the coefficients in Eqs. (61) and (62). Blue and light blue circles correspond to the minimum of effective MQ and ED polarizability accounting for cross-multipole coupling, respectively. Blue and light blue squares correspond to the same spectral point as circles and indicate $|\alpha_p^{\text{eff}}| = |\alpha_p^{\text{eff,coup}}|$ and $|\alpha_M^{\text{eff}}| = |\alpha_M^{\text{eff,coup}}|$, respectively. (b) Inverse MQ polarizability and cross-multipole coupling sum. (c) Inverse ED polarizability and cross-multipole coupling sum. In (b) and (c), blue and light blue circles correspond to the same spectral points as the circles in (a). Here all electric dipole and quadrupole polarizabilities are divided on ε_0.
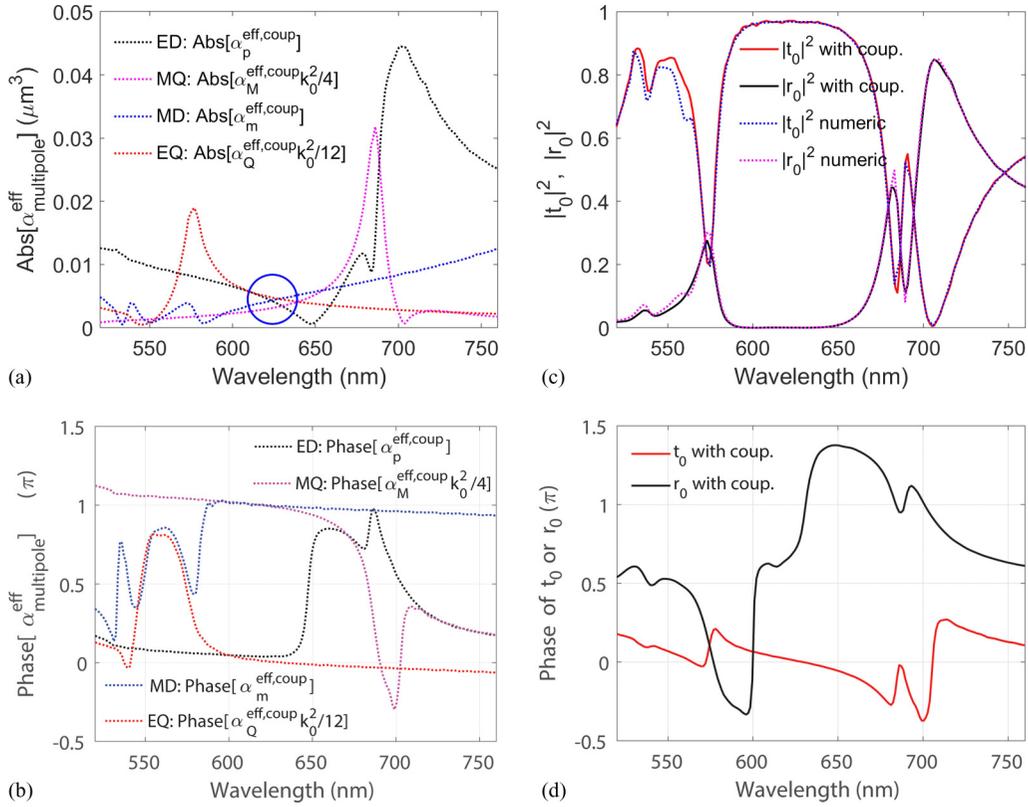
FIG. 7. Multipole resonances and reflection and transmission through the periodic array of spheres. The lattice periods are $D_x = 530$ nm and $D_y = 410$ nm, and silicon particles have $R = 125$ nm. (a) Absolute values of each separate multipole term in the brackets of Eqs. (61) and (62) for the reflection and transmission coefficients (the MQ and EQ effective polarizabilities are normalized to $k_0^2/4$ and $k_0^2/12$, respectively, and ED and EQ polarizabilities are divided on ε_0). (b) Corresponding phases of the multipole terms in Eqs. (61) and (62). (c) Intensity reflection and transmission coefficients. (d) Phase of field reflection and transmission coefficients (61) and (62). At the wavelength 610–630 nm, the contributions of multipole moments in the reflection and transmission coefficients have comparable values; the phases of ED and EQ terms are almost equal to each other, and the same holds for MD and MQ. At this wavelength range, reflection is near zero, transmission is close to 1 and its phase does not change, indicating a lattice anapole state.

excitation of a certain multipole combination in the nanoparticles of the metasurface. This multipole combination provides simultaneous strong minimization of forward and backward scattering of light resulting in its propagation almost without amplitude or phase change. Note that such behavior can be called the "lattice anapole effect" because of its similarity to the light scattering by particles in anapole states [53]. In these states, nanoparticles do not scatter light, providing the unperturbed incident wave. Here we show that the lattice anapole effect can be realized in an array of spherical silicon nanoparticles due to interference of the fields generated by ED, MD, EQ, and MQ moments excited in the array's nanoparticles. For this, we perform calculations for a periodic array of silicon spheres with periods $D_x = 530$ nm and $D_y = 410$ nm (Fig. 7). The spectral region of interest is the wavelength internal 610–630 nm indicated by a blue circle in Fig. 7(a). There, all four multipole terms in the brackets of expressions (61) and (62) have comparable values. At the same time in this spectral region, the phases of the ED and EQ terms are almost equal to zero, and the phases of the MD and MQ terms are close to π [Fig. 7(b)]. Using the information about the amplitudes and phases of the polarizability terms in the field reflection and transmission coefficients, we obtain from (61) and (62) that $r_0 \approx 0$ and $t_0 \approx 1$ in the considered wavelength range

610–630 nm. Direct numerical and analytical calculations of the intensity reflection and transmission coefficients shown in Fig. 7(c) confirm this result: The reflection from the array is near zero, and the transmission is close to 1. Moreover, the phase change of the transmitted wave is almost equal to zero [the red curve in Fig. 7(d) for wavelengths from 610 to 630 nm]. Calculations of the field distribution at $\lambda = 629$ nm, where transmission is close to unit and the phase change is zero, confirm that the wave propagates through the array unperturbed [Figs. 8(a) and 8(b)]. Contrarily, for the wavelength $\lambda = 580$ nm, the phase of the transmission field changes, and one can see a significant reflection from the array and a phase shift of the transmitted wave compared with the free-space case [Figs. 8(c) and 8(d)]. Note that from a comparison of the analytical and numerical curves presented in Fig. 7(c), one can see that the analytical model taking into account only ED, MD, EQ, and MQ multipole terms can describe well the optical properties of the arrays under consideration. Thus, we have designed the array of spherical silicon nanoparticles where the propagating light excites moderate resonances (offset from resonance peaks) but is not reflected, and the light transmits almost with the same amplitude as the incident light and without phase changes. As a result, this behavior can be associated with a lattice anapole state.
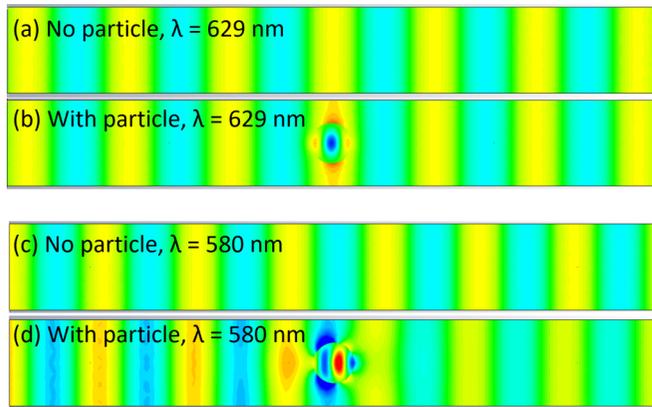
FIG. 8. Total E_x field distribution (incident and scattered waves) in numerical simulations of (a),(c) an empty domain and (b),(d) a domain with a sphere in the array with $D_x = 530$ nm and $D_y = 410$ nm. Simulations are performed at the wavelength (a),(b) $\lambda = 629$ nm (which corresponds to the transmission phase $\phi = 0$ and the lattice anapole state) and (c),(d) $\lambda = 580$ nm. Light incidence is from the left side. A cross section is taken in the xz plane.

V. CONCLUSION

A general case of nanoparticles and their array with the electric and magnetic dipole and quadrupole moments has been theoretically considered. Equations that include the contribution of the MQ moment and the MQ Green's tensor for the description of electromagnetic fields generated by the MQ moment in all wave zones are derived. We have developed an analytical model based on coupled dipole-quadrupole equations for the investigation of the optical responses of nanoparticle arrays supporting dipole and quadrupole (including the MQ term) resonances. Further, the developed model has been applied for the study of optical properties of infinite periodic arrays of identical silicon spheres. An analytical expression of the effective particle polarizabilities, taking into account multipole coupling, has been obtained. Performing calculations with the developed analytical model, we demonstrated the importance of the coupling effects between ED and MQ moments in the infinite arrays. It has been shown that excitation of all dipole and quadrupole moments in the silicon nanosphere arrays can lead to the realization of a lattice anapole state. This state corresponds to a condition when particle resonances are excited, but neither the amplitude nor the phase of the transmitted wave changes. Thus, we believe that the presented analytical model can be used for the development and investigation of nanoparticle structures with different functional optical properties.

[1] H. A. Atwater and A. Polman, Plasmonics for improved photovoltaic devices, Nat. Mater. **9**, 205 (2010).

[2] P. Offermans, M. C. Schaafsma, S. R. K. Rodriguez, Y. Zhang, M. Crego-Calama, S. H. Brongersma, and J. G. Rivas, Universal scaling of the figure of merit of plasmonic sensors, ACS Nano **5**, 5151 (2011).

[3] I. Staude, A. E. Miroshnichenko, M. Decker, N. T. Fofang, S. Liu, E. Gonzales, J. Dominguez, T. S. Luk, D. N. Neshev, I. Brener, and Y. Kivshar, Tailoring directional scattering through magnetic and electric resonances in subwavelength silicon nanodisks, ACS Nano **7**, 7824 (2013).

[4] Y. F. Yu, A. Y. Zhu, R. Paniagua-Domnguez, Y. H. Fu, B. Lukyanchuk, and A. I. Kuznetsov, High-transmission dielectric metasurface with 2π phase control at visible wavelengths, Laser Photon. Rev. **9**, 412 (2015).

[5] M. Decker, I. Staude, M. Falkner, J. Dominguez, D. N. Neshev, I. Brener, T. Pertsch, and Y. S. Kivshar, High-efficiency dielectric Huygens surfaces, Adv. Opt. Mater. **3**, 813 (2015).

[6] S. V. Zhukovsky, V. E. Babicheva, A. B. Evlyukhin, I. E. Protsenko, A. V. Lavrinenko, and A. V. Uskov, Giant Photogalvanic Effect in Noncentrosymmetric Plasmonic Nanoparticles, Phys. Rev. X **4**, 031038 (2014).

[7] V. E. Babicheva, S. Gamage, M. I. Stockman, and Y. Abate, Near-field edge fringes at sharp material boundaries, Opt. Express **25**, 23935 (2017).

[8] E. Prodan, C. Radloff, N. J. Halas, and P. Nordlander, A hybridization model for the plasmon response of complex nanostructures, Science **302**, 419 (2003).

[9] B. Luk'yanchuk, N. I. Zheludev, S. A. Maier, N. J. Halas, P. Nordlander, H. Giessen, and C. T. Chong, The Fano resonance in plasmonic nanostructures and metamaterials, Nat. Mater. **9**, 707 (2010).

[10] A. B. Evlyukhin, C. Reinhardt, A. Seidel, B. S. Luk'yanchuk, and B. N. Chichkov, Optical response features of Si-nanoparticle arrays, Phys. Rev. B **82**, 045404 (2010).

[11] P. D. Terekhov, K. V. Baryshnikova, Y. A. Artemyev, A. Karabchevsky, A. S. Shalin, and A. B. Evlyukhin, Multipolar response of nonspherical silicon nanoparticles in the visible and near-infrared spectral ranges, Phys. Rev. B **96**, 035443 (2017).

[12] V. E. Babicheva, Directional scattering by the hyperbolic-medium antennas and silicon particles, MRS Adv. **3**, 1913 (2018).

[13] A. Alu and N. Engheta, Achieving transparency with plasmonic and metamaterial coatings, Phys. Rev. E **72**, 016623 (2005).

[14] P. C. Mundru, V. Pappakrishnan, and D. A. Genov, Material- and geometry-independent multishell cloaking device, Phys. Rev. B **85**, 045402 (2012).

[15] D. A. Genov and P. C. Mundru, Quasi-effective medium theory for multi-layered magneto-dielectric structures, J. Opt. **16**, 015101 (2014).

[16] J. Y. Lee, A. E. Miroshnichenko, and R.-K. Lee, Simultaneously nearly zero forward and nearly zero backward scattering objects, Opt. Express **26**, 30393 (2018).

[17] A. B. Evlyukhin, C. Reinhardt, and B. N. Chichkov, Multipole light scattering by nonspherical nanoparticles in the discrete dipole approximation, Phys. Rev. B **84**, 235429 (2011).

[18] M. Kerker, D. Wang, and C. Giles, Electromagnetic scattering by magnetic spheres, J. Opt. Soc. Am. **73**, 765 (1983).

[19] Y. H. Fu, A. I. Kuznetsov, A. E. Miroshnichenko, Y. F. Yu, and B. Lukyanchuk, Directional visible light scattering by silicon nanoparticles, Nat. Commun. **4**, 1527 (2013).

[20] S. Person, M. Jain, Z. Lapin, J. J. Saenz, G. Wicks, and L. Novotny, Demonstration of zero optical backscattering from single nanoparticles, Nano Lett. **13**, 1806 (2013).

[21] J. van de Groep and A. Polman, Designing dielectric resonators on substrates: Combining magnetic and electric resonances, Opt. Express **21**, 26285 (2013).

[22] K. V. Baryshnikova, M. I. Petrov, V. E. Babicheva, and P. A. Belov, Plasmonic and silicon spherical nanoparticle antireflective coatings, Sci. Rep. **6**, 22136 (2016).

[23] V. Babicheva, M. Petrov, K. Baryshnikova, and P. Belov, Reflection compensation mediated by electric and magnetic resonances of all-dielectric metasurfaces, J. Opt. Soc. Am. B **34**, D18 (2017).

[24] V. E. Babicheva and A. B. Evlyukhin, Resonant suppression of light transmission in high-refractive-index nanoparticle metasurfaces, Opt. Lett. **43**, 5186 (2018).

[25] B. Lamprecht, G. Schider, R. T. Lechner, H. Ditlbacher, J. R. Krenn, A. Leitner, and F. R. Aussenegg, Metal Nanoparticle Gratings: Influence of Dipolar Particle Interaction on the Plasmon Resonance, Phys. Rev. Lett. **84**, 4721 (2000).

[26] B. Auguie and W. L. Barnes, Collective Resonances in Gold Nanoparticle Arrays, Phys. Rev. Lett. **101**, 143902 (2008).

[27] W. Wang, M. Ramezani, A. I. Vakevainen, P. Torma, J. G. Rivas, and T. W. Odom, The rich photonic world of plasmonic nanoparticle arrays, Mater. Today **21**, 303 (2018).

[28] V. G. Kravets, A. V. Kabashin, W. L. Barnes, and A. N. Grigorenko, Plasmonic surface lattice resonances: A review of properties and applications, Chem. Rev. **118**, 5912 (2018).

[29] S. Zou, N. Janel, and G. C. Schatz, Silver nanoparticle array structures that produce remarkably narrow plasmon lineshapes, J. Chem. Phys. **120**, 10871 (2004).

[30] V. A. Markel, Divergence of dipole sums and the nature of non-Lorentzian exponentially narrow resonances in one-dimensional periodic arrays of nanospheres, J. Phys. B **38**, L115 (2005).

[31] W. Zhou, M. Dridi, J. Y. Suh, C. H. Kim, D. T. Co, M. R. Wasielewski, G. C. Schatz, and T. W. Odom, Lasing action in strongly coupled plasmonic nanocavity arrays, Nat. Nanotechnol. **8**, 506 (2013).

[32] S. V. Zhukovsky, V. E. Babicheva, A. V. Uskov, I. E. Protsenko, and A. V. Lavrinenko, Enhanced electron photoemission by collective lattice resonances in plasmonic nanoparticle-array photodetectors and solar cells, Plasmonics **9**, 283 (2014).

[33] S. V. Zhukovsky, V. E. Babicheva, A. V. Uskov, I. E. Protsenko, and A. V. Lavrinenko, Electron photoemission in plasmonic nanoparticle arrays: Analysis of collective resonances and embedding effects, Appl. Phys. A **116**, 929 (2014).

[34] B. D. Thackray, P. A. Thomas, G. H. Auton, F. J. Rodriguez, O. P. Marshall, V. G. Kravets, and A. N. Grigorenko, Super-narrow, extremely high quality collective plasmon resonances at telecom wavelengths and their application in a hybrid graphene-plasmonic modulator, Nano Lett. **15**, 3519 (2015).

[35] S. D. Swiecicki and J. E. Sipe, Surface-lattice resonances in two-dimensional arrays of spheres: Multipolar interactions and a mode analysis, Phys. Rev. B **95**, 195406 (2017).

[36] S. D. Swiecicki and J. E. Sipe, Periodic Green functions for 2D magneto-electric quadrupolar arrays: Explicitly satisfying the optical theorem, J. Opt. **19**, 095006 (2017).

[37] A. B. Evlyukhin, C. Reinhardt, U. Zywietz, and B. N. Chichkov, Collective resonances in metal nanoparticle arrays with dipole-quadrupole interactions, Phys. Rev. B **85**, 245411 (2012).

[38] V. E. Babicheva and A. B. Evlyukhin, Resonant lattice Kerker effect in metasurfaces with electric and magnetic optical responses, Laser Photon. Rev. **11**, 1700132 (2017).

[39] C. Y. Yang, J. H. Yang, Z. Y. Yang, Z. X. Zhou, M. G. Sun, V. E. Babicheva, and K. P. Chen, Nonradiating silicon nanoantenna metasurfaces as narrow-band absorbers, ACS Photon. **5**, 2596 (2018).

[40] V. E. Babicheva and A. B. Evlyukhin, Metasurfaces with electric quadrupole and magnetic dipole resonant coupling, ACS Photon. **5**, 2022 (2018).

[41] V. E. Babicheva and A. B. Evlyukhin, Interplay and coupling of electric and magnetic multipole resonances in plasmonic nanoparticle lattices, MRS Commun. **8**, 712 (2018).

[42] W. Liu and Y. S. Kivshar, Generalized Kerker effects in nanophotonics and meta-optics, Opt. Express **26**, 13085 (2018).

[43] A. B. Evlyukhin, T. Fischer, C. Reinhardt, and B. N. Chichkov, Optical theorem and multipole scattering of light by arbitrarily shaped nanoparticles, Phys. Rev. B **94**, 205434 (2016).

[44] O. Keller, Attached and radiated electromagnetic fields of an electric point dipole, J. Opt. Soc. Am. B **16**, 835 (1999).

[45] O. J. F. Martin and N. B. Piller, Electromagnetic scattering in polarizable backgrounds, Phys. Rev. E **58**, 3909 (1998).

[46] P. Morse and H. Feschbach, *Methods of Theoretical Physics* (Feshbach, Minneapolis, 2005).

[47] A. B. Evlyukhin, C. Reinhardt, E. Evlyukhin, and B. N. Chichkov, Multipole analysis of light scattering by arbitrary-shaped nanoparticles on a plane surface, J. Opt. Soc. Am. B **30**, 2589 (2013).

[48] C. P. Burrows and W. L. Barnes, Large spectral extinction due to overlap of dipolar and quadrupolar plasmonic modes of metallic nanoparticles in arrays, Opt. Express **18**, 3187 (2010).

[49] C. F. Bohren and D. R. Huffman, *Absorption and Scattering of Light by Small Particles* (Wiley Interscience, New York, 1983).

[50] V. A. Markel, Comment on "Silver nanoparticle array structures that produce remarkably narrow plasmon line shapes" [J. Chem. Phys. 120, 10871 (2004)], J. Chem. Phys. **122**, 097101 (2005).

[51] P. D. Terekhov, V. E. Babicheva, K. V. Baryshnikova, A. S. Shalin, A. Karabchevsky, and A. B. Evlyukhin, Multipole analysis of dielectric metasurfaces composed of nonspherical nanoparticles and lattice invisibility effect, Phys. Rev. B **99**, 045424 (2019).

[52] E. Palik, *Handbook of Optical Constant of Solids* (Academic, San Diego, 1985).

[53] A. E. Miroshnichenko, A. B. Evlyukhin, Y. F. Yu, R. M. Bakker, A. Chipouline, A. I. Kuznetsov, B. Luk'yanchuk, B. N. Chichkov, and Y. S. Kivshar, Nonradiating anapole modes in dielectric nanoparticles, Nat. Commun. **6**, 8069 (2015).